Article

# Experimental and numerical studies on detonation wave propagating in a rectangular tube with obstacles

Hiroyuki Sato*†, Nobuyuki Tsuboi**, A. Koichi Hayashi*, and John H. S. Lee ***

*Department of Mechanical Engineering, Aoyama Gakuin University, 5-10-1 Fuchinobe, Sagamihara, Kanagawa 229-8558, JAPAN
†corresponding author: sato@me.aoyama.ac.jp

**Japan Aerospace Exploration Agency (JAXA), 3-1-1 Yoshinodai, Sagamihara, Kanagawa 229-8510, JAPAN

***Department of Mechanical Engineering, McGill University, 845 Sherbrooke St. W. Montreal, Quebec, H3A 2K6, CANADA

Received: May 10, 2004　Accepted: July 28, 2004

## Abstract
When detonation propagates in a tube with obstacles or with variable sections, it is fundamentally an important issue to elucidate how detonation fails and re-initiates in such a tube. In the present study experiments and numerical simulation are performed to investigate mechanisms of failure and re-initiation of detonation propagation in obstacled tubes. First of all, numerical simulation is validated by comparing data with experiments to analyze propagation mechanism of detonation in obstacled tubes. Two different obstacle configurations, staggered and symmetrical array, are used to see detonation failure and re-initiations. As the result, it is found that detonation failure occurs when it collides with obstacles to become expansion waves and re-initiations behind combustion wave fronts for both staggered and symmetrical cases. Jet ignition promotes fast deflagration transition to detonation in the symmetrical obstacle configurations.

## 1. Introduction
As for the application of detonation phenomena, one of topics is to develop the system of pulse detonation engine (PDE). For the utilization of PDE, it comes out of an ideally detonation wave called C-J detonation. An important factor to develop such the system is to examine DDT (deflagration to detonation transition) phenomena. Urtiew and Oppenhim [1] visualized DDT in stoichiometric hydrogen-oxygen mixtures with very clear Schlieren photographs and classified the DDT phenomena into four modes. Studies on the propagation of detonation waves in a very rough walled tube or a tube filled with obstacles were carried out by Chapman and Wheeler [2], Shchelkhin [3], and Guenoche [4] in the 1920's through 40's. This problem was taken up again in the 70's and 80's by Lee and co-worker who first referred to quasi-steady supersonic combustion wave as "quasi-detonation waves" or "fast deflagration waves" since their propagating velocities can be substantially below that of the normal C-J detonation velocity of the mixture. Teodorczyk et al. [5), 6)] proposed that the propagation mechanisms of the quasi-detonation wave are due to quenching and re-initiation of detonation through shock reflection from the wall. The limit criterion is based on relationship between blockage ratio of the obstruction and cell size of detonation (e.g., Peraldi et al. [7)] and Gu et al. [8)]). Ohyagi et al. [9)] observed the interaction of detonation waves on the tube wall with obstacles. The wave structures of the quasi-detonations as well as the shock-deflagration wave complex were observed.

In order to clarify the DDT phenomena, especially a combustion wave propagating in DDT condition, the present study shows detonation propagating mechanism in an obstacled array, and some detailed mechanism of detonation failure and re-initiation based on the results of experiment and numerical simulation.

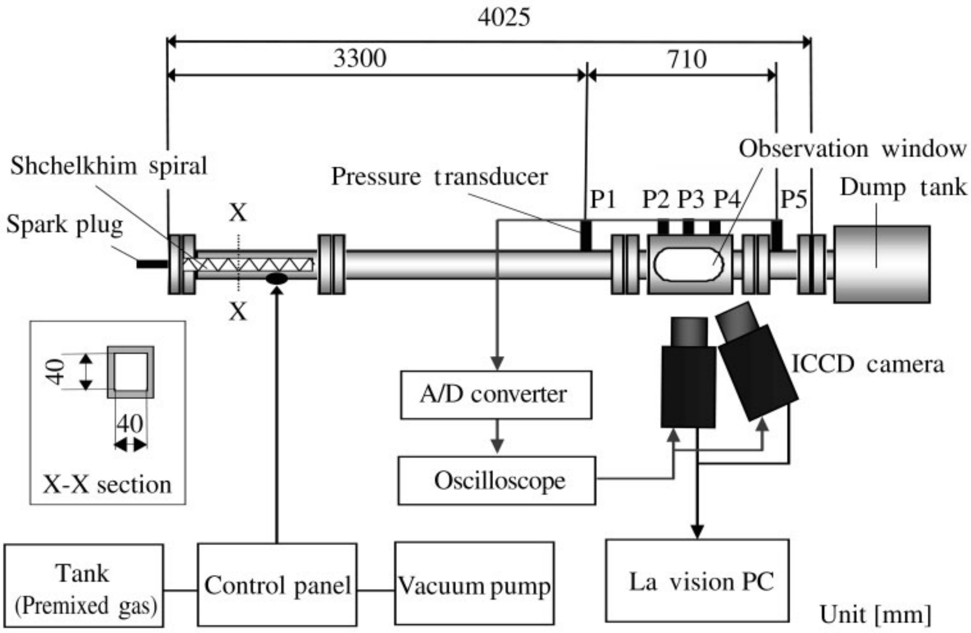


Fig. 1 Experimental setup and measurement system.

## 2. Experimental setup

Figure 1 shows a schematic of the experimental apparatus. The tube used in this experiment has a 40×40mm rectangular cross-section and a length of 4025mm. Obstacles is equipped on plates and they are also fixed in the tube. Figure 2 shows a dimension of the obstacles. The spacing between the obstacles $i$ is 60mm and the width of the obstacles $w$ is 4mm. The heights of the obstacles $h$ are 4mm and 8mm. This study arranges these obstacles plates as shown in Fig. 3.

The propagation velocity and pressure are measured with pressure transducers (PCB113A24) and embedded in sidewalls, namely at P1 (3300mm from the diaphragm), P2 (365mm from P1), P3 (425mm from P1), P4 (485mm from P1), and P5 (710mm from P1). The direct emission photographs are obtained by using two ICCD cameras (LaVision NanoStar). The frame intervals are 10μs. Soot-track records are obtained on a thin soot-coated aluminum plate fixed in place of the observation window. The test gases are stoichiometric hydrogen-air mixtures at initial pressure of 101.3kPa. In order to get a shorter DDT distance, a Shchelkhin spiral of 500mm in length is used at the driver section near the spark plug.

## 3. Numerical method

Numerical computations have also been performed by integrating one-dimensional and two-dimensional Euler equations with Petersen and Hanson model [10] (hydrogen - air of 9 species and with 18 reactions including high-pressure 3rd body reactions). Difference for the convective term is calculated using a non-MUSCL modified-flux type TVD-upwind scheme and time difference using a 2nd-order Strang-type fractional step method. Especially we treat a chemical reaction by a point implicit way to get stable calculation. Initial condition is obtained by patching a one-dimensional detonation data at the upstream of numerical region of 1.0×7.0mm (the grid size is 5μm×10μm) and keeping the downstream as 101.3kPa and 298.15K. It pro-

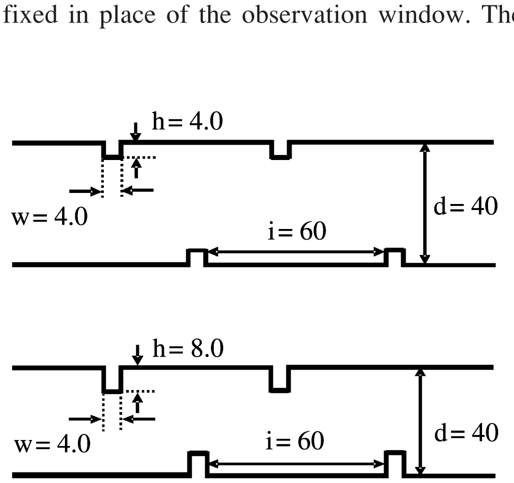


Fig. 2 Obstacles configurations for experiments.

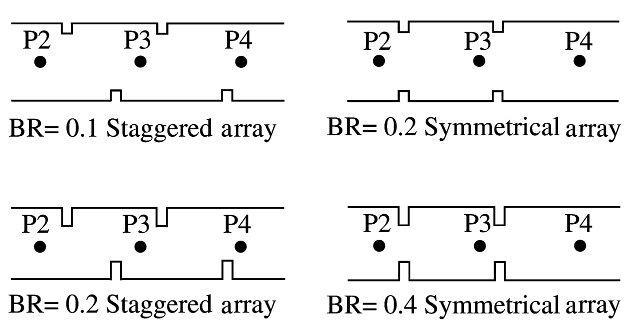


Fig. 3 Obstacles arrangements.

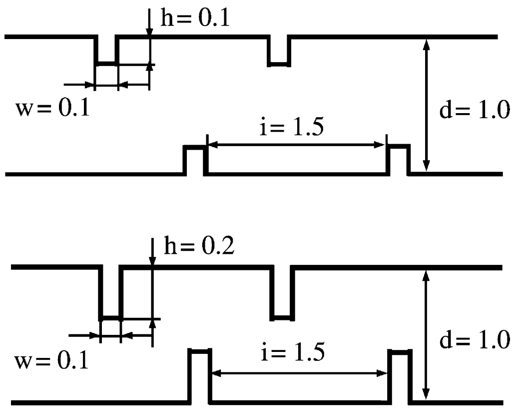


Fig. 4 Obstacles configurations for numerical simulation.

vides different one-dimensional initial data for 2D calculation. As for the boundary conditions, the wall condition including obstacles is mirror condition and the downstream condition is flowing out one. Figure 4 shows the size of obstacles. Obstacles arrangements are the same as shown in Fig. 3.

## 4. Results and discussion

An overall mechanism of detonation propagation in the obstacled tube is studied through experimental results and some detailed mechanisms are shown by numerical simulations which are clarified by comparing with experimental data. Especially, it is investigated where and how combustion wave is re-ignited. Two obstacle systems, staggered and symmetrical arrangements, are examined from the detonation propagation point of view.

### 4.1 Comparison between experimental data and numerical results

In order to compare numerical results with experimental ones, a similarity in size is considered in the present analysis by keeping the blockage ratio (geometrical factor) and equivalence ratio of the mixture of hydrogen and air. The width of the tube in numerical simulation is 1mm comparing with that of 40mm in experiments and the number of triple points in the test section is one in numerical simulation rather than 4-6 in experiments. This difference in the number of triple points may provide the different conclusion, however fortunately, once detonation hits an obstacle, more or less triple points disappear; i.e., its cellular structure collapses, and only a combustion wave appears until it hits obstacles. From this point of view, the comparison of numerical analyses with experiments is worth to study.

Figures 5 and 6 show the direct emission taken by ICCD camera experimentally and temperature profiles picked up near obstacles with the numerical results, respectively. If the radiation by heat release closely corresponds to temperature, both profiles seem to be compared. In the staggered array (see. Fig. 3), both experimental and numerical configurations of reflected shock wave after detonation hits the obstacle, and re-initiation point on the wall are agreed each other. Those reflected shock waves are strong enough to propagate upstream. On the other hand, in the symmetrical obstacle formation, a strong radiation provides a diamond structure of shock interaction in both the experiment and numerical simulation. Although the detail comparison of physical values between experiments and numerical simulations is not obtained, those data imply the qualitative value of numerical simulation.

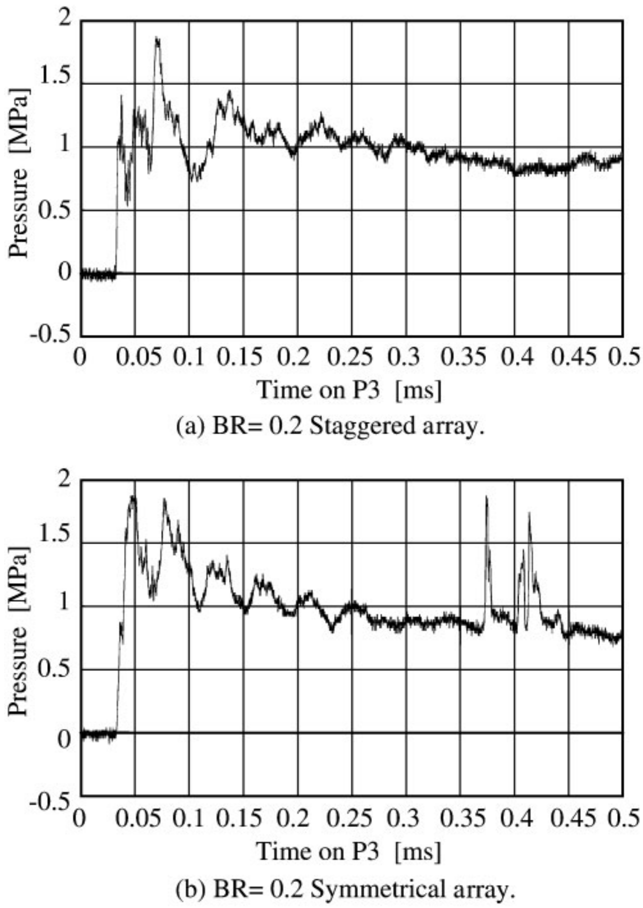


Fig. 7 Experimental pressure records on P3.

Instead of comparing between experimental and numerical pressure profiles, experimental results of cell pattern appeared in the soot-coated tube, which correspond to the high-pressure peaks as the dynamics of transverse wave, are compared to numerical pressure profiles in 2D plane. The sequential pressure records at the position of P3 (see. Fig. 3) are shown in Fig. 7. These pressure profiles show the break-up of detonation structure to become combustion waves in both the staggered and symmetrical array cases. However, as seen in Fig. 7-(b) of the symmetrical array case, at certain time later the apparent re-initiation is observed in the pressure profile at P3 and the same tendency is recognized in the numerical pressure profiles (see. Fig. 8-(b)). This is one of DDT cases and is caused by the reflected shock wave interactions. Another remark is that the overall pressure in the whole flow field do not decrease substantially probably due to the interactions of shocks and combustion wave with obstacles.

The numerical pressure profiles picked up near obstacles for the staggered and symmetrical arrays are shown in Fig. 8. The main important findings in Fig. 8 is that re-initiations are observed everywhere by the interaction among reflected shock waves from obstacles. The staggered array case gives lots of the re-initiation points, which correspond to the high-pressure regions, comparing with the result of the symmetrical array case due to the effect of the transverse wave. The symmetry of obstacle configuration provides obviously more or less symmetric propagation structure of combustion wave.

From those studies of comparing the experimental results with numerical ones, numerical simulation performed in the present study will have an accuracy to predict detonation propagation mechanism in the obstacled tube.

### 4.2 Detonation failure

One of the main purposes in the present study is to clarify how detonation fails or re-ignites in the obstacled tube. In this section, it is studied from the experimental and numerical results how detonation propagates in obstacled tube. First, OH radical mass fraction profiles are used to understand the mechanism of detonation failure and re-initiation and the second, detonation failure is also studied from the experimental measurement of velocity and numerical data through two different types of obstacle configurations; staggered and symmetrical types.

Figures 9 and 10 show the OH radical mass fraction profiles picked up near obstacles obtained numerically. Figures 9-(a) and 9-(b) correspond to the case of BR=0.1, that of BR=0.2, respectively. Figures 10-(a) and 10-(b) correspond to the case of BR=0.2, that of BR=0.4, respectively. As described in the previous section, when detonation collides with the obstacle, the triple points disappear and detonation becomes fast deflagration, but in any case there exist re-initiations behind the combustion wave front where OH radicals increase. This comes from the interaction among reflected transverse waves with obstacles as seen in pressure (see. Fig. 8) and temperature (see. Fig. 6)

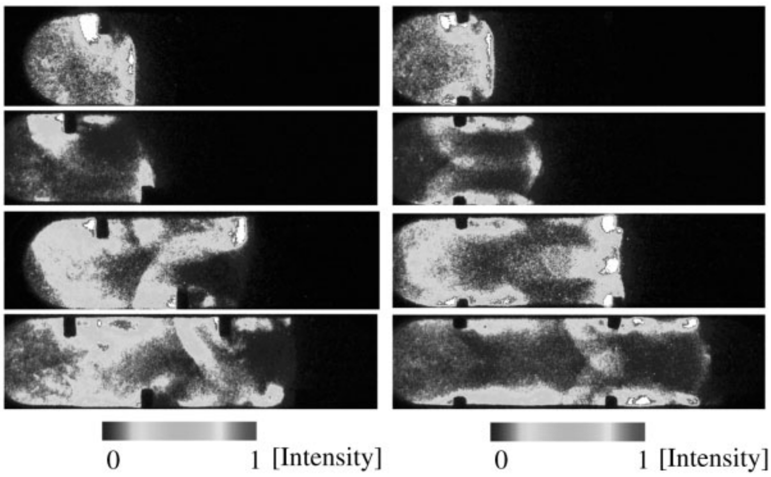


(a) BR= 0.2 Staggered array. (b) BR= 0.2 Symmetrical array.

Fig. 5 Experimental direct emission photographs.

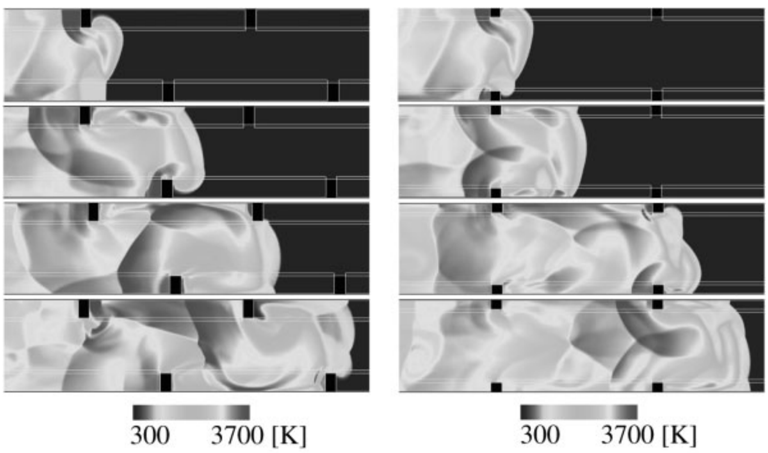


(a) BR= 0.2 Staggered array. (b) BR= 0.2 Symmetrical array.

Fig. 6 Numerical temperature profiles.

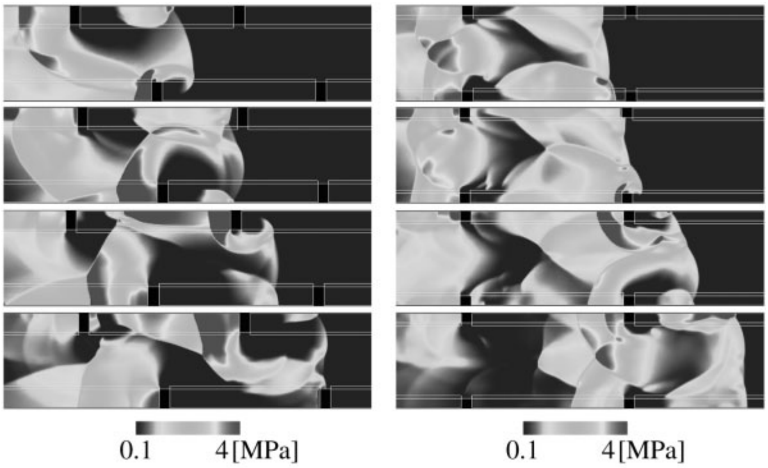


(a) BR= 0.2 Staggered array. (b) BR= 0.2 Symmetrical array.

Fig. 8 Numerical pressure profiles.

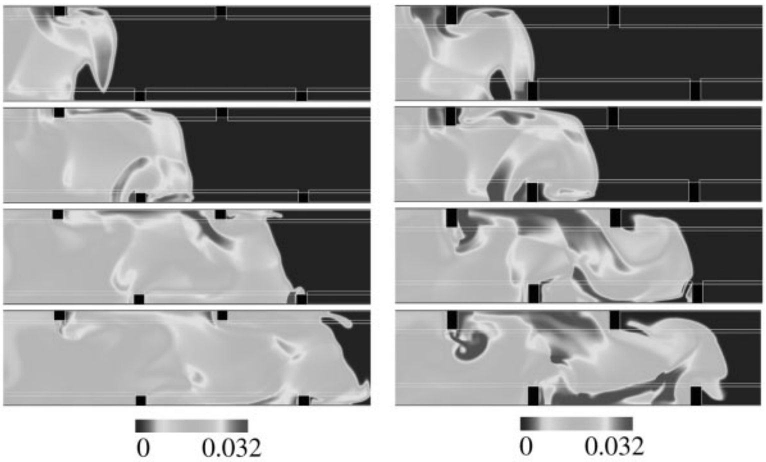


(a) BR= 0.1 Staggered array. (b) BR= 0.2 Staggered array.

Fig. 9 Numerical OH radical mass fraction profiles on staggered array.

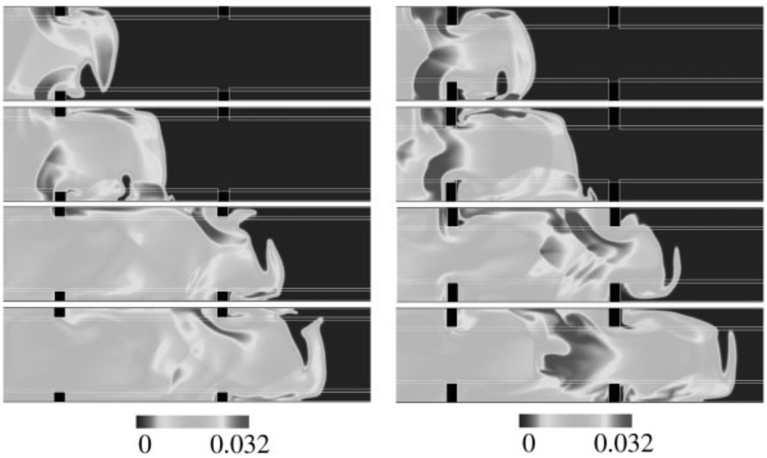


(a) BR= 0.2 Symmetrical array. (b) BR= 0.4 Symmetrical array.

Fig. 10 Numerical OH radical mass fraction profiles on symmetrical array.

profiles. The re-initiation will also come from the interaction of the transverse wave with walls. However, in the present case those re-initiations do not give the combustion wave to catch up with the wave front to be detonation. Other findings show that the fast deflagration is accelerated by the symmetrical array blockages rather than the staggered ones.

Figure 11 is to plot the measured detonation velocity along the obstacled tube, which corresponds to the cases of OH mass fraction profiles. As far as this result, the effect of blockages works on detonation in the staggered array case better than that in the symmetrical array case. The feature in detonation propagation in the symmetrical array case is the jet initiation which gives a strong initiation and thrust to the fast deflagration.

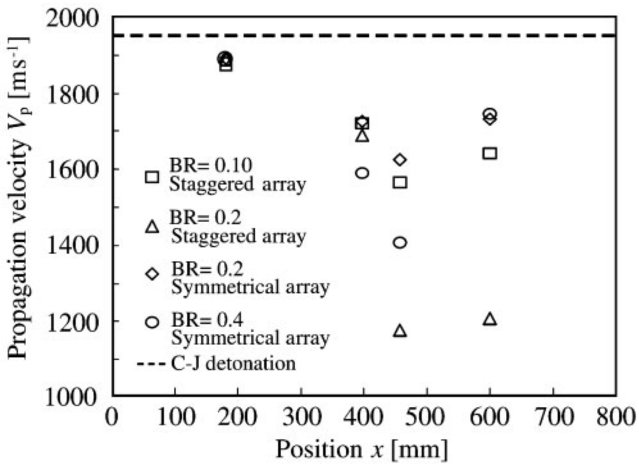


Fig. 11 Propagation velocities (experiment).

## Concluding remarks

Detonation propagation mechanism in the obstacled tube is studied experimentally and numerically to clarify the followings:

- Although the size of considered region is different between the experiment and numerical simulation, the simulation using a detailed chemical reaction model gives the qualitative result which is the similar to the behavior of combustion wave observed with the experiment.
- Two types of obstacle array, the staggered and symmetrical, are examined to show the different detonation propagating mechanisms. The staggered array provides the detonation failure and the symmetrical one does the recovery to detonation by jet initiation.

## Acknowledgement

This work was supported by Prof. Fumio Higashino. We would also like to thank Mr. Keisuke Asami who graduated at Aoyama Gakuin University, Satoshi Shiokawa, Hiroyuki Jotaki and Junta Misawa who are Aoyama Gakuin University students for their help on our investigation.

## References

1) P. A. Urtiew, A. K. Oppenheim, Proc. Roy. Soc. London Ser. A, Vol.295, pp. 13-28, 1966.
2) W. R. Chapman and R. V. Wheeler, J. Chem. Soc. (London), 2139, 1926.
3) I. I. Shchelkhin, J.E.P.T. (USSR) 10, 823, 1940.
4) H. Guenoche and N. Manson, Revue de l'institut Francais du Petrole, No. 2, pp. 53-69, 1949.
5) A. Teodorczyk, J. H. S. Lee and R. Knystautas, Proc. 22nd Symp. (Int.) on Combustion, The Combustion Institute, pp. 1723-1731, 1988.
6) A. Teodorczyk, J. H. S. Lee and R. Knystautas, Proc. 23rd Symp. (Int.) on Combustion, The Combustion Institute, pp. 735-741, 1990.
7) O. Peraldi, R. Knystautas and J. H. S. Lee, Proc. 21st Symp. (Int.) on Combustion, The Combustion Institute, pp. 1629-1637, 1986.
8) L. S. Gu, R. Knystautas and J. H. S. Lee, Proc. 11th Int. Colloq. On Dynamics of Explosions and Reactive Systems, Warsaw, August, 1987.
9) S. Ohyagi, T. Obara, P. Cai, T. Yoshihashi and Y. Kuroda, 23rd Symp. (Int.) on Shock Waves, pp. 180-186, 2001.
10) L. Petersen and K. Hanson, Journal of propulsion and power Vol.15, No.4, July-August, 1999.